Analysis of Stray Flux Spectral Components in Induction Machines under Rotor Bar Breakages at Various Locations

P. A. Panagiotou, I. Arvanitakis, N. Lophitis, J. A. Antonino-Daviu, K. N. Gyftakis

***Abstract* -- Induction machines under rotor electrical faults have been subjected to intensive research over the years. It is not only the nature of the fault that makes it important to study, but also the differences observed regarding this fault's effect on the motor's conditions. One of these conditions is the rotor bar breakages at non adjacent positions, which has drawn the attention of researchers due to the false negative diagnostic alarms that may be caused. In this paper, a novel approach is presented aiming to reliably detect this type of fault condition. The proposed method is based on the analysis of specific subcomponents of the stray flux over time. The analysis is implemented on an industrial 1.1 MW industrial induction motor, since large industrial motors make the cases where MCSA might fail due to the weak speed ripple effect and closeness of the fault's sidebands to the fundamental harmonic. The work has been carried out with extensive Finite Element simulations.**

***Index Terms*-- broken bars, induction motor, signal processing, spectral content, stray flux**

I. Introduction

The fact that induction machines have taken over the majority of industrial applications in the modern world, has risen the demand of efficient and reliable monitoring methods. This demand has been served over the years with different efficient monitoring techniques combined with diagnostic methods and Finite Element Analysis (FEA), using measurements of either stator currents or voltages, speed or torque ripples and magnetic field related quantities [1]-[4]. The latter case has been developed during the last years, making use of modern signal processing methods to assess fault conditions during both the start-up transient, and the steady state [5], [6].

Competing more and more with the conventional Motor Current Signature Analysis (MCSA), the Stray Flux Signature Analysis (SFSA) has been applied with success for various types of faults [7]-[11]. For this type of analysis, magnetic flux that strays outside the motor is monitored by capturing the voltage induced on rigid search coils, sized inversely proportional to the machine's height [7], [10]. This allows searching for signatures in the frequency spectra, according to the origin of stray flux, thus being axial flux [7], axial & radial flux [8]-[10] or pure radial flux [11].

In the aforementioned works, rotor related, stator related and supply related fault signatures have been thoroughly studied, for space and time dependent harmonics. The detection of such signatures is based on the early as well as recent studies for condition monitoring, in which the theoretical, experimental and quantitative modelling of the harmonic and spectral content is provided [4]-[6], [12]-[15].

Focusing on rotor electrical faults, rotor cage defects have been examined in [12] with the use a multi-equational numerical model, evaluating the $(1-2s):f_s$ component inefficient for some locations of a random broken bar fault. The broken bar sidebands are also examined in [13] taking advantage of the sideband modulus as a relative indicator accounting for the speed-ripple effect, while [14] introduces an analytical categorization of harmonics for different case studies of healthy cages. An interesting comparison of signal spectral analysis methods is also given by [15] for broken bar faults, using observers and providing a descriptive analysis of internal and external diagnostic methods. An analytical approach for the stator related frequencies under bar breakages provides [16], investigating the upper and lower sidebands of the 1st, 5th and 7th harmonic experimentally, and a comprehensive review of advanced diagnostics and methods for fault detection is given in [17].

Extensive research for the position and non-adjacency of the bar breakages has been undertaken as well [18]-[25]. The reason for this interest lies in the fact that the physical mechanisms of these faults evolve undetected and they vary for real condition industrial case scenarios, as they can depend on the machine design and rotor construction [2], [4], [20]-[21]. As explained in [18] using a simplified model, non-adjacent broken bars can lead to misdiagnosis or masking of the fault, when two faulty bars are located within half pole pitch, leading to false negative diagnosis. The same work addresses, that when multiple odd breakages are spotted within one complete pole's pitch, the fault could be partially masked as a case with broken bars at adjacency. A similar analysis is provided in [19], examining the case where bars with breakage are in cross-diametrical positions for a four pole induction machine.

The influence of non-successive breakages on MCSA implementation and reliability is examined in [20] by the

Panagiotis A. Panagiotou is with Faculty of Engineering, Environment and Computing, and Research Institute Future Transport & Cities, Coventry University, UK (e-mail: panagio4@uni.coventry.ac.uk).

Ioannis Arvanitakis is with School of Computing, Electronics and Mathematics, Coventry University, UK (e-mail: ac7632@coventry.ac.uk).

Neophytos Lophitis is with the Research Institute Future Transport & Cities and the Faculty of Engineering, Environment and Computing, Coventry University (e-mail: n.lophitis@coventry.ac.uk).

Jose A. Antonino-Daviu is with the Instituto Tecnológico de la Energía, Universitat Politècnica de València, Valencia, Spain (e-mail: joanda@die.upv.es).

Konstantinos N. Gyftakis is with the Research Institute Future Transport & Cities and the School of Computing, Electronics and Mathematics, Faculty of Engineering, Environment and Computing, Coventry University, UK (e-mail: k.n.gyftakis@ieee.org).

978-1-5386-2477-7/18/$31.00 ©2018 IEEE

application of the fault current approach and space-vector theory. Also, in [21] the authors reliably detect rotor asymmetries, using signal decomposition during the transient regime, in cases of industrial applications diagnosed as false-negative with MCSA. Furthermore, in [22] and [23] the diagnostic potential of the zero sequence current (ZSC) is validated for cases of broken bars being adjacent and not respectively, while [24] introduces an indicator for detection of non-serial breakages using the Filtered Park's Vector Approach (FPVA). A compelling evaluation of high-order fault related harmonics is delivered by [25] for cases of double bar faults.

Regarding the methods for signal analysis during machine operation, advanced signal processing techniques based on the time-frequency decomposition (TFD) have been proposed in the recent years [26]-[33]. These techniques provide the representation of a signal on the joint time-frequency plane, allowing its decomposition, in order to study frequency transitions in time and observe oscillatory harmonic components and how they evolve. These include the Discrete Wavelet Decomposition (DWT) [21], [27] or the same technique using complex wavelets [28], while high-resolution spectral analysis techniques like the MUSIC algorithm have also been proposed [29].

To the same direction, a reconfigurable monitoring device is presented in [30], aiming for diagnosis of industrial equipment through application of DWT and Short-Time Fourier Transform (STFT). The latter is successfully used in [31], combined with notch filters, for detection of lubrication and bearing faults. The STFT is also utilized in [32] for speed estimation through the current space vector amplitudes fluctuation, as well as in [33] for an approach on the same basis. Although it holds the drawback of a relatively reduced frequency resolution [29], the STFT is frequently preferred due to its simplicity in terms of low computational complexity and commercial availability in software packages.

In this work, the behaviors of the stray flux spectral components of a 6-pole squirrel-cage induction motor with nominal characteristics 6.6 kV, 1.1 MW, 50Hz are analyzed and studied using 2D FEM. Under healthy condition and suffering from various adjacent and non-adjacent broken bars, the STFT is employed for the representation of the stray flux spectral content on the T-F plane by means of the spectrogram. As a second step, since these trajectories respond as periodical oscillations in time, their spectral densities calculated by the STFT are highlighted. Then, the normalized FFT is examined for all cases of healthy and faulty motors. The aim is to observe the frequency content of the trajectories at steady state and draw a conclusion regarding their behavior and response in time and frequency domain, hence investigate how the fault frequencies carried in the signal of stray flux are modulated when the fault occurs in non-consecutive positions.

II. Theoretical Background

A. Radial SFSA & Broken Bar Fault Signatures

A series of works have handled the application of radial stray flux measurement [8]-[11]. The medium frequency emission harmonic components and the physical mechanisms causing them are extensively described in [11] for a broken bar and one inter-turn short circuit. Similar approach, focusing on the low frequency components is introduced in [35] for examination of eccentricity and broken bar faults. The same rotor faults are studied in [36]-[38] using internal Hall-effect flux sensors, providing an assiduous analytical description of the air-gap flux space harmonics. Also, stray flux signature analysis is applied for bar breakages in [39] & [40].

When a bar breakage occurs, a backward rotating magnetic field is generated due to the open-circuited bar and the lack of inter-bar and eddy currents in the point of breakage, creating in the rotor cage an asymmetry that is clearly reflected in the motor's harmonic content [6], [11], [35]-[38]. This fault asymmetry is known to cause additional frequency sidebands, distanced by multiples of the motor's slip s from the fundamental frequency f_s and its multiples [21], [36]. These appear in the spectrum of stator-related quantities (stator current or stray flux), modulated by the component $(1-s)f_s$ because of induction from the rotor to the stator and vice-versa. The equation for these fault related sideband signatures is the following [36], [37]:

$$f_{bb} = [k/p(1-s) \pm s]:f_s \,, \qquad (1)$$

p being the number of pole pairs and k/p an integer.

The problem is that in large induction motors, like the one under analysis in this paper, these fault signature sidebands lie very close to the fundamental frequency because of the rotor's speed being very close to the synchronous one, thus the low value of slip s at steady state [38]. Another similar issue is explained in [41], for cases where the load-torque ripple sidebands are approximately equal to the $2sf_s$ sidebands. These facts can complicate the diagnostic process and make it very difficult to detect the fault with accuracy, especially in the classical FFT analysis where the spectral leakage of the windowing function is already an issue to encounter. Therefore, the sideband signatures of the 5th and 7th harmonic will be investigated in this work, since they are standing off at the distances $-4sf_s$ and $-6sf_s$ for the 5th and at $-6sf_s$ and $-8sf_s$ for the 7th harmonic.

B. The Short-Time Fourier Transform

As introduced in the previous Section (I), the STFT offers a time-frequency representation of a signal by picturing the signals' spectral characteristics over time. The frequencies' spectral energy density is visualized by the spectrogram, which yields a contour plot of the magnitude. The contour plot is color-coded in a scale that expresses the intensity of the signal's spectral energy magnitude [31]-[33].

The continuous time STFT $X(t, f)$ of a signal is a function of both time t and frequency f – as opposed to the classical FFT that represents the signals' harmonic content as a function of frequency only – that can be computed from the FFT over a sliding window by the following equation [34]:

$$X(t,f) = \int_{-\infty}^{+\infty} x(t)w(t-\tau)e^{-j2\pi ft}dt \,, \quad (2)$$

where $x(t)$ is the signal of our interest, $w(t)$ is the sliding window, τ is the window shifting factor and $f=2\pi/\omega$ the frequency. Equation (2) provides the joint time-frequency representation, as previously discussed, by means of the spectrogram:

$$S(t, f) = |X(t, f)|^2 \qquad (3).$$

III. FEM Modelling & Spectral Components

A. The FEM models

For this analysis, an industrial Y-connected, 6-pole, 6.6 kV, 1.1 MW, 50 Hz cage induction motor was simulated with MagNet software from Infolytica. Having the exact geometrical and materials characteristics provided by the manufacturer, the rotor has been designed with 70 copper bars and the stator with 54 slots and a double layer 12-turn per slot 1 to 9 pitched winding. The healthy motor is depicted in Fig. 1a and the corresponding magnetic field in Fig. 1b. A brief description of the modelled motor is given in Table I.

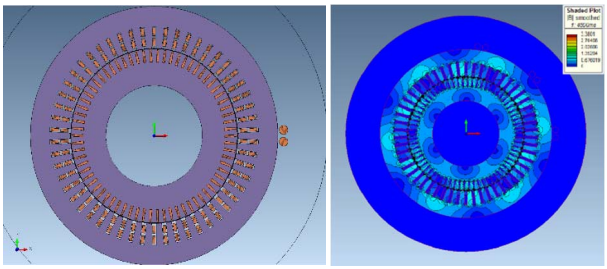

a) b)

Fig. 1. a) Healthy motor and b) magnetic field distribution of healthy motor.

TABLE I
SIMULATION CHARACTERISTICS OF THE MOTOR UNDER STUDY

Characteristics	***Value***
Supply frequency f_s	50 Hz
Stator connection	Y
Output power	1.1 MW
Rated Voltage	4.6 kV
Rated Current	170 A
Number of poles	6
Rated speed	990 rpm
Number of stator slots	54
Number of rotor bars	70

Besides the healthy motor, four more cases have been simulated and studied accounting for different cage breakages: a case of two adjacent broken bars, two cases of non-adjacent broken bars and the last case of two adjacent combined with a non-adjacent one. All motors serve the same mechanical load 11kNm at steady state.

To aid the reader, the five distinct FEM cases are labeled and referred to as Case #1 to #5. The cases are summarized in Table II along with the value of slip for each one of them, and the motors under the broken bar fault with the asymmetry in the corresponding magnetic flux density distribution are shown in Fig. 2.

TABLE II
THE CASE STUDIES

Case	***Broken Bars***	***Location***	***Slip (%)***
#1	Healthy	-	0.91
#2	1 & 2	Adjacent	0.95
#3	1 & 6	Within half pole pitch	0.96
#4	1 & 11	Within one pole pitch	0.94
#5	1, 2 & 11	Combination of Cases #2 and #4	0.98

The flux sensor is a stranded 50-turn search coil, with the input and output wounded on a point of the machine's periphery close to the stator frame (Fig. 1a).

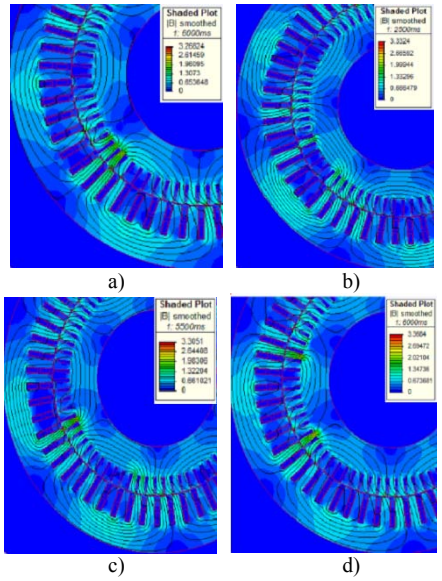

a) b) c) d)

Fig. 2. Motors under simulation & analysis: a) Case #2, b) Case #3, c) Case #4 and d) Case #5.

From Fig. 2, one can see that the broken bar fault asymmetry is not easily distinguished and observed in the magnetic field distribution for Case #3 and Case #4. The opposite is observed for Case #2 and Case #5, which comes in agreement with the observations stated in [18] for the fault taking place at such positions. In addition, the FFT on the radial stray flux signal of Case #1 (blue), Case #2 (red) and Case #3 (black) is shown in Fig. 3-a for the frequency area around the fundamental 50 Hz harmonic, where the closeness of the broken bar sidebands to f_s is noted. Fig. 3-b shows the STFT around the same frequency area, pointing the difficulty to observe the sidebands on the T-F plane because of their small distance from f_s and its spectral leakage overlap.

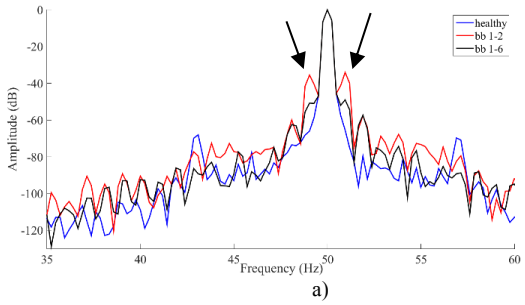

a)

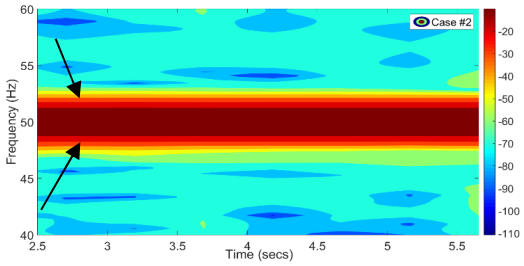

b)

Fig. 3. a) FFT of Case #1 (blue), Case #2 (red) and Case #3 (black) and b) STFT of Case #2 in the frequency area of the fundamental f_s.

B. *The Spectral Components*

For the analysis of the studied signals, the discrete time STFT is implemented [34]. A Kaiser window of length L=9216 is selected as the sliding window function, with parameter $\beta = 40$ and *80%* overlap between the time-frames. This ad-hoc selection accrued from fine tuning of the parameters accounting for two factors: firstly, to achieve a windowing with a response as close as possible to rectangular, and secondly to yield a good trade-off between time and frequency resolution, in order to observe the signals' harmonic trajectories in the spectrogram [15], [31].

Because of the low slip value and the problem of spectral leakage described previously, focus will be given to the sidebands of the higher harmonics at 250 Hz (5th harmonic) and 350 Hz (7th harmonic). In order to individualize the $(5\text{-}4s)f_s$ and $(5\text{-}6s)f_s$ components and the $(7\text{-}6s)f_s$ and $(7\text{-}8s)f_s$ components, the average value of slip at steady state is used, as well as the spectrograms shown in Fig. 4.

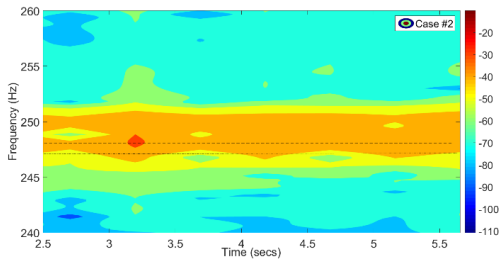

a)

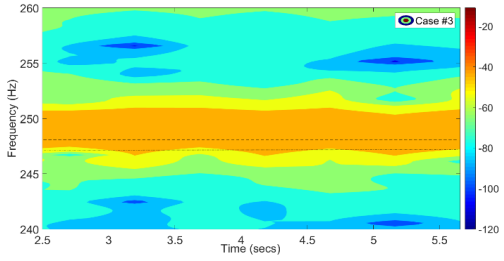

b)

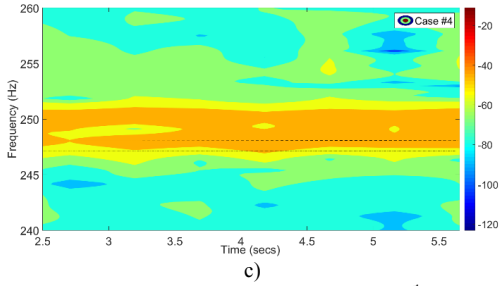

c)

Fig. 4. STFT Spectrogram for the frequency area of the 5th harmonic for: a) Case #2, b) Case #3 and c) Case #4.

In the spectrograms of Fig. 4, the frequency components are pointed with dashed lines. The broken bar fault related components are used to derive from Eq. 3 their spectral content as follows:

$$S(t, f_{o,i}) = |X(t, f_{o,i})|^2, \qquad (4)$$

for each component $f_{o,i}$ of interest.

For a better visualization, Fig. 5 depicts the spectrogram of the stray flux for Case #5, in the frequency areas of the 5th (Fig. 5-a) and 7th harmonic (Fig. 5-b) as well.

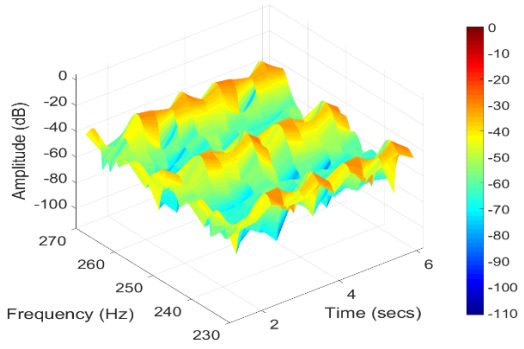

a)

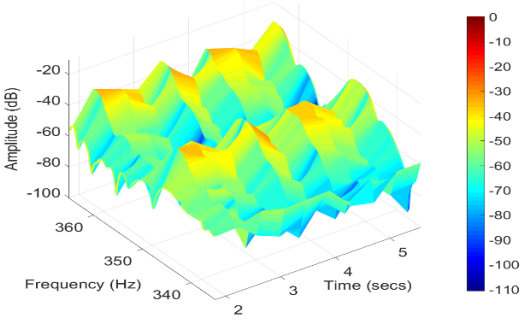

b)

Fig. 5. STFT Spectrogram of Case #5 for the frequency area of: a) the 5th harmonic and b) the 7th harmonic.

The localized frequencies of Table III are extracted and evaluated in the time and frequency domain to observe how they are modulated.

IV. Results & Analysis

As a next step, to characterize these modulations, the FFT is applied to each calculated time-signal $S(t, f_{o,i})$ of each case, considering the part of the signal that belongs to the steady state $(t \geq 1\ sec)$. The signals are shown in Fig. 6 for the 5th and 7th harmonics' sidebands of all cases.

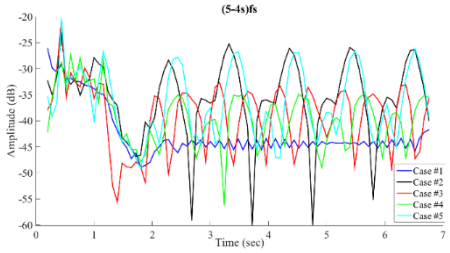

a)

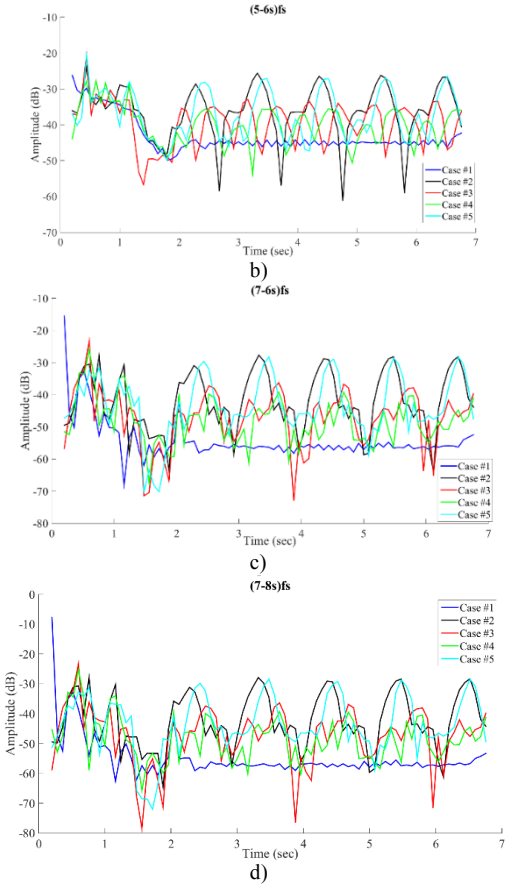

Fig. 6. The time-signals $S(t, f_{o,i})$ for all cases at the frequencies: a) *(5-4s)fs*, b) *(5-6s)fs* c) *(7-6s)fs* c) *(7-6s)fs*.

A first observation noted from Fig. 6 for all cases, is that the frequency components of the healthy motor are characterized by small amplitudes, compared to the faulty cases. Also, these frequencies behave as mono-component signals, with no significant oscillations and without carrying any slow evolving frequency components. This is not the case for the motors with broken bars though, where it is clearly observed that a dilatory frequency is included in the main signal and which is indicative for the presence of a rotor related fault.

Furthermore, Fig. 7 and Fig. 8 depict the corresponding FFT spectra of each signal $S(t, f_{o,i})$ from Fig. 6, for all cases at the 5th and 7th harmonic, respectively. The amplitudes of all components under investigation are summarized in Tables III and IV.

An inspection of the spectra in Fig. 7 provides a straight forward indication that a rotor fault has occurred, since the amplitudes of the faulty motors are at -20 dB, having increased 30 dB with respect to the healthy motor, which is stabilized at approximately -50 dB. Also, the FFT spectra of Fig. 7 reveal a spectral signature at 2 Hz (red arrows). This signature practically corresponds to the $-4sf_s$ sideband, where all the faulty cases have the same amplitude. This is an important observation, since the fault indicator at this frequency is showing the same result about the fault, regardless of the position of the broken bars. Similar is the behavior of the component at $-6sf_s$, which is illustrated at 3 Hz (black arrows), where the faulty models approach an amplitude of -30 dB. At this frequency, Case #2 makes the only exception, where the signature's amplitude is erected at a maximum level, because of the breakage adjacency that creates a larger local magnetic field asymetry.

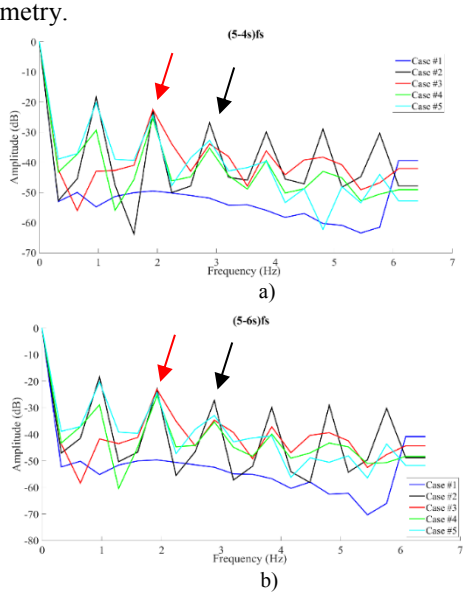

Fig. 7. FFT spectra of each $S(t, f_{o,i})$ for all cases for the spectral components of: a) *(5-4s)fs* and b) *(5-6s)fs*.

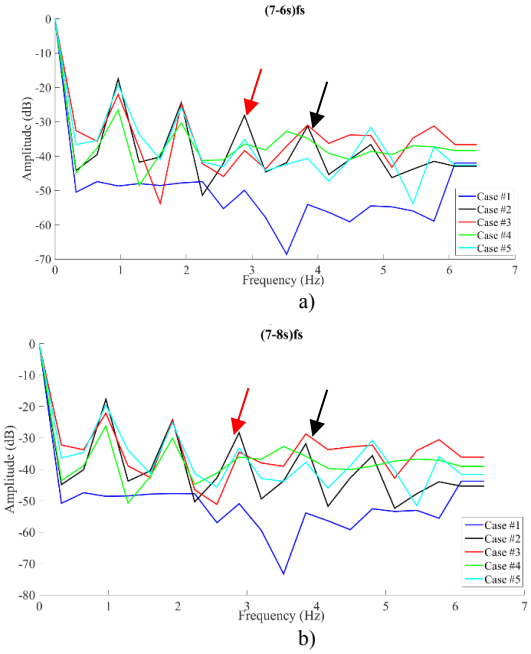

Fig. 8. FFT spectra of each $S(t, f_{o,i})$ for all cases for the spectral components of: a) *(7-6s)fs* and b) *(7-8s)fs*.

TABLE III
AMPLITUDES OF THE 5TH HARMONIC COMPONENTS

Case	2 Hz	3 Hz
	$5fs - 4sf_s$	$5f_s - 6sf_s$
1	-50	-52.38
2	-22.79	-27.21
3	-22.79	-34.62
4	-25.35	-35.26
5	-24.34	-32.86

TABLE IV
AMPLITUDES OF THE 7TH HARMONIC COMPONENTS

Case	3 Hz	4 Hz
	$7f_s - 6sf_s$	$7f_s - 8sf_s$
1	-50	-53.8
2	-28.11	-31.85
3	-38.34	-28.7
4	-36.45	-35.82
5	-35.14	-37.79

Examination of Fig. 8 aims to harvest information about the fault through the $-6sf_s$ component at 3 Hz (red arrows) and the component $-8sf_s$ at 4 Hz (black arrows). Both frequencies depicted in Fig. 8-a and Fig. 8-b are affected by the $-6sf_s$ component, reaching an amplitude increase of 20 dB with respect to the healthy motor. Again, the case of adjacent broken bars exceeds all other amplitudes, having increased 5 dB more than all other cases.

Finally, it is interresting how the two frequencies of Fig. 8 respond to the $-8sf_s$ commponent, which fails to reliably detect the combined broken bar fault of Case #5, but surprisingly gives a satisfying alarm level for the fault occuring at the distance of half pole pitch (Case #3) and one complete pole pitch (Case #4).

V. DISCUSSION & FUTURE WORK

In this work, a new approach is introduced for the detection of rotor electrical faults through the examination of frequency spectral components, extracted from the time-frequency representation of the radial stray flux signal. Focus was given on the 5th and 7th harmonics' sidebands, due to their relative further distance from the central harmonic. Having extracted their spectral density $S(t, f_o)$ with use of the Short-Time Fourier Transform, these signals at each chosen frequency were again represented in the time domain to observe how their amplitudes respond in time and examine how they are modulated.

Implementation of the classical FFT on each time-signal $S(t, f_o)$ at steady-state offered inspection of subcomponent signatures of frequencies located at $2ksf_s$ for each corresponding harmonic, whose behavior seems to be designated according to the impact of the speed-ripple caused by the broken bar asymmetry. The component related to the $-4sf_s$ sideband is reported reliable enough for broken bar diagnosis, independently from the position of the fault. Similar behavior is reported for the $-8sf_s$ component, which only fails to diagnose a combined rotor fault of two adjacent broken bars and a non-adjacent one.

Ongoing and future work in this matter aims to proceed with combination of this method with a filtering technique to achieve improved localization of trajectories on the T-F plane, and potentially enhancement of the FEM results with experimental verification of similar broken bar cases.

VI. REFERENCES

[1] M. S. Elricki, Y. Porat, A. Alexandrovitz, "Leakage Field Changes of an Induction Motor as Indication of Nonsymmetric Supply", *IEEE Transactions on Industry and General Applications*, Vol. IGA-7, No. 6, Nov/Dec 1971.

[2] N. M. Elkasabgy, A. R. Eastham, G.E. Dawson, "The Detection of Broken Bars In The Cage Rotor of an Induction Machine", *Conference Record of the IEEE Industry Applications Society (IAS) Annual Meeting,* pp. 181-187, Vol. 1, 1988.

[3] G. B. Kliman, R. A. Koegl, J. Stein, R. D. Endicott, M. W. Madden, "Noninvasive Detection of Broken Rotor Bars in Operating Induction Motors", *IEEE Transactions on Energy Conversion,* Vol. 3, No. 4, pp. 873-89, Dec 1988.

[4] A. Bellini, F. Flippetti, G. Franceschini, C. Tassoni, G. B. Kliman, "Quantitative Evaluation of Induction Motor Broken Bars By Means of Electrical Signature Analysis", *Conference Record of the Thirty-First Annual Meeting and World Conference on Industrial Applications of Electrical Energy,* pp. 484-491, Vol. 1, 2000.

[5] H. Henao, T. Assaf, G. A. Capolino, "Detection of Voltage Source Dissymmetry in an Induction Motor Using the Measurement of Axial Leakage Flux", *International Conference on Electrical Machines (ICEM),* Aug 2000.

[6] M. El H. Benbouzid, G. B. Kliman, "What Stator Current Processing-Based Technique to Use for Induction Motor Rotor Faults Diagnosis?", *IEEE Transactions on Energy Conversion,* Vol. 18, No. 2, pp. 238-244, June 2003.

[7] T. Assaf, H. Henao, G. A. Capolino, "Simplified Axial Flux Spectrum Method to Detect Incipient Stator Inter-Turn Short-Circuits in Induction Machine", *IEEE International Symposium on Industrial Electronics,* pp. 815-819, 2004.

[8] A. Yazidi, H. Henao, G. A. Capolino, "Broken Rotor Bars Fault Detection in Squirrel Cage Induction Machines", *IEEE International Conference on Electric Machines and Drives,* pp. 741-747, 2005.

[9] S. H. Kia, H. Henao, G. A. Capolino, C. Martis, "Induction Machine Broken Bars Fault Detection Using Stray Flux after Supply Disconnection", *IEEE IECON-32nd Annual Conference on Industrial Electronics,* pp. 1498-1503, 2006.

[10] A. Yazidi, H. Henao, G. A. Capolino, M. Artioli, F. Filippetti, D. Casadei, "Flux Signature Analysis: an Alternative Method for the Fault Diagnosis of Induction Machines", *IEEE Russia Power Tech,* pp. 1-6, 2005.

[11] R. Romary, R. Corton, D. Thailly, J. F. Brudny, "Induction Machine Fault Diagnosis Using an External Radial Flux Sensor", *The European Physical Journal-Applied Physics*, 32 (2), pp. 125-132, 2005.

[12] Tadeusz J. Sobczyk, Waclaw Maciolek, "Is the $(1-2s)f_0$ in Sator Currents Sufficient for Detection of Rotor Cage Faults?", *IEEE International Symposium on Diagnostics for Electric Machines, Power Electronics and Drives (SDEMPED),* Vienna, Austria, pp.1-5, Sep. 2005.

[13] A. Bellini, C, Concari, G. Franceschini, E. Lorenzani, C. Tassoni, A. Toscani, "Thorough Understanding and Experimental Validation of Current Sideband Components in Induction Machines Rotor Monitoring", *IEEE IECON - 32nd Annual Conference on Industrial Electronics,* pp. 4957-4962, 2006.

[14] G. M. Joksmovic, J. Riger, T. M. Wolbank, N. Peric, M. Vasak, "Stator-Current Spectrum Signature of Healthy Cage Rotor Induction Machines", *IEEE Transactions on Industrial Electronics,* Vol. 60, No. 9, pp. 4025-4033, 2013.

[15] M. Eltabach, A, Charara, I. Zein, "A Comparison of External and Internal Methods of Signal Spectral Analysis for Broken Rotor bars Detection in Induction Machines", *IEEE Transactions on Industrial Electronics,* Vol. 51, No. 1, pp. 107-121, 2004.

[16] H. Henao, H. Razik, G.A. Capolino, "Analytical Approach of the Stator Current Frequency Harmonics Computation for Detection of Induction Machine Rotor Faults", *IEEE Transactions on Industry Applications,* Vol. 41, No. 3, pp. 801-807, 2005.

[17] A. Bellini, F. Filippetti, C. Tassoni, G.A. Capolino, "Advances in Diagnostic Techniques for Induction Machines", *IEEE Transactions on Industrial Electronics",* Vol. 55, No. 12, pp. 4109-4126, 2008.

[18] G. Y. Sizov, A. Sayed-Ahmed, C.C. Yeh, N. A. O. Demerdash, "Analysis and Diagnostics of Adjacent and Nonadjacent Broken-Rotor-Bar Faults in Squirrel-Cage Induction Machines", *IEEE Transactions on Industrial Electronics,* Vol. 56, No. 11, pp. 4627-4641, 2009.

[19] A. Menacer, G. Champenois, M. S. Nait Said, A. Benakcha, S. Moreau, S. Hassaine, "Rotor Failures Diagnosis of Squirrel Cage Induction Motors with Different Supplying Sources", *Journal of Electrical Engineering & Technology,* Vol. 4, No. 2, pp. 219-228, 2009

[20] M. Riera-Guasp, M. Fernandez Cabanas, J. A. Antonino-Daviu, M. Pineda-Sanchez, C. H. Rojas Garcia, "Influence of Nonconsecutive Bar Breakages in Motor Current Signature Analysis for the Diagnosis of

Rotor Faults In Induction Motors", *IEEE Transactions on Energy Conversion,* Vol. 25, No. 1, pp. 80-89, 2011.
[21] J.A. Antonino-Daviu, S.B. Lee, E. Wiedenbrug, "Reliable detection of rotor bar failures in induction motors operating in petrochemical plants", IEEE Petroleum and Chemical Industry Conference Europe, pp. 1-9, 2014.
[22] K. N. Gyftakis, J. A. Antonino-Daviu, R. Garcia-Hernandez, M. McCulloh, D. A. Howey, A. J. Marques-Cardoso, "Comparative Experimental Investigation of Broken Bar Fault Detectability in Induction Motors", *IEEE Transactions on Industry Applications*, Vol. *52*, No. 2, pp. 1452-1459, 2016
[23] J. A. Antonino-Daviu, K. N. Gyftakis, R. Garcia-Hernandez, H. Razik, A. J. Marques-Cardoso, "Comparative Influence of Adjacent and Non-adjacent Broken Rotor Bars on the Induction Motor Diagnosis trough MCSA and ZSC Methods", *IEEE IECON,* pp. 001680-001685, 2015
[24] K. N. Gyftakis, J. A. Antonino-Daviu, A. J. Marques-Cardoso, "A Reliable Indicator to Detect Non-Adjacent Broken Rotor Bars Severity in Induction Motors", IEEE XXII International Conference on Electrical Machines (ICEM), pp. 2910-2916, 2016.
[25] M. Riera-Guasp, J. Pons-Linares, F. Vedreno-Santos, J. A. Antonino-Daviu, M. Fernandez Cabanas, "Evaluation of the Amplitudes of High-Order Fault Related Components in Double Bar Faults", *IEEE International Symposium on Diagnostics for Electric Machines, Power Electronics and Drives (SDEMPED),* pp. 307-315, 2011.
[26] J. A. Antonino-Daviu, V. Climente-Alarcon, J. Pons-Linares, M. Pineda-Sanchez, P. Jover-Rodriguez, A. Arkkio, "Application of TFD tools for the tracing of eccentricity-related components in induction machines", *IECON'09, IEEE 35th Annual Conference of Industrial Electronics,* pp. 1039-1044*,* 2009.
[27] S. H. Kia, H. Henao, G. A. Capolino, "Diagnosis of Broken-Bar Fault in Induction Machines Using Discrete Wavelet Transform Without Slip Estimation", *IEEE Transactions on Industry Applications,* Vol. 45, No. 4, pp. 1395-1404, 2009.
[28] I. P. Tsoumas, G. Georgoulas, E. D. Mitronikas, A. N. Safacas, "Asynchronous Machine Rotor Fault Diagnosis Technique Using Complex Wavelets", *IEEE Transactions on Energy Conversion,* Vol. 23, No. 2, pp. 444-459, 2008.
[29] A. Garcia-Perez, R. J. Romero-Troncoso, E. Cabal-Yepez, R. A. Osornio-Rios, Jose de Jesus Rangel-Magdaleno, H. Miranda, "Startup Current Analysis of Incipient Broken Rotor Bar in Induction Motors using High-Resolution Spectral Analysis", *IEEE International Symposium on Diagnostics for Electric Machines, Power Electronics and Drives (SDEMPED),* pp. 657-663, 2011.
[30] E. Cabal-Yepez, A. G. Garcia-Ramirez, R. J. Romero-Troncoso, A. Garcia-Perez, R. A. Osornio-Rios, "Reconfigurable Monitoring System for Time-Ferquency Analysis on Industrial Equipment Through STFT and DWT", *IEEE Transactions on Industrial Informatics,* Vol. 9, No. 2, pp. 760-71, 2013.
[31] M. Lopez-Ramirez, R. J. Romero-Troncoso, D. Morinigo-Sotelo, O. Duque-Perez, L. M. Ledesma-Carrillo, D. Camarena-Martinez, A. Garcia-Perez, " Detection and Diagnosis of Lubrication and Faults in Bearing on Induction Motors through STFT", IEEE 2016 International Conference on Electronics, Communications and Computers (CONIELECOMP), pp. 13-18, 2016.
[32] C. Wang, Z. Zhou, P. J. Unsworth, P. Igic, "Current Space Vector Amplitude Fluctuation based Sensorless Speed Measurement of Induction Machines Using Short Time Fourier Transformation", *IECON'09, IEEE 35th Annual Conference of Industrial Electronics,* pp. 1869-1874, 2008.
[33] C. Wang, Z. Zhou, P.J. Unsworth, T. O'. Farrell, "Sensorless Speed Measurement of Induction Machines Using Short Time Fourier Transformation", *IEEE International Symposium on Power Electronics, Electrical Drives, Automation and Motion (SPEEDAM)*, pp. 1114-1119, 2008.
[34] K. Gröchenig. "Foundations of time-frequency analysis", Springer Science & Business Media, *2013*.
[35] A. Ceban, R. Pusca, R. Romary, "Eccentricity and Broken Rotor Bars Faults – Effects on the External Axial Field", *XIX IEEE International Conference on Electrical Machines (ICEM),* pp. 1-6, 2010
[36] K. Saad, G. Mirzaeva, "Fault Diagnosis of Induction Motors by Space Harmonics Analysis of the Main Air Gap Flux", *IEEE ICEM* '14, pp. 1608-1613, 2014.
[37] K. Saad, G. Mirzaeva, "Advanced Diagnosis of Rotor Faults in Large Induction Motors Based on Internal Flux Measurement", *IEEE IAS Annual Meeting,* pp. 1-8, 2016.
[38] K. Saad, G. Mirzaeva, "Space-Time Representation of the Main Air Gap Flux of a Three Phase Squirrel Cage Induction Motor and its Application to Detect Eccentricity", *IEEE International Electric Machines and Drives Conference (IEMDC),* 2015.
[39] I. Chernyavska, O. Vitek, "Analysis of Broken Rotor Bar Fault in a Squirrel-Cage Induction Motor by Means of Stator Current and Stray Flux Measurement", *IEEE International Power Electronics and Motrion Control Conference (PEMC),* pp. 532-537, 2016.
[40] P. Bernat, Z. Hytka, P. Kacor, "Indication of failures of rotor bar on induction machine with squirrel cage rotor in its external electromagnetic field", *IEEE 16th* International Scientific Conference on Electric Power Engineering (EPE), pp. 691-696, 2015.
[41] C. Concari, G. Franceschini, C. Tassoni, "Induction machine current space vector features to effectively discern and quantify rotor faults and external torque ripple", *IET* Electric Power Applications, Vol. 6, No. 6, pp. 310-321, 2012.

VII. BIOGRAPHIES

Panagiotis A. Panagiotou was born in Thessaloniki, Greece, in 1989. He received the 5 year Diploma in Electrical & Computer Engineering from the University of Patras, Greece, in 2015 and the MSc in Complex Systems & Network Theory from Aristotle University of Thessaloniki, Department of Mathematics in 2016. Currently, he is a Ph.D Candidate at Coventry University, UK. His research is focused on condition monitoring and fault diagnosis of electric motors for industrial and EV applications, as well as statistical modelling and signal processing for diagnostic purposes.

Ioannis Arvanitakis received his 5 year Diploma in Electrical & Computer Engineering from University of Patras, Greece in 2009, and his Ph.D. from the same institution in 2017, entitled "Navigation and Collaborative Mapping of a Team of Mobile Robots". He is currently an Assistant Lecturer at Coventry University, UK. His main research interests include Navigation, Guidance and Control, Obstacle Avoidance algorithms, Unmanned Ground Vehicles, Simultaneous Localization and Mapping (SLAM) algorithms, Nonlinear Modeling, Optimization Theory.

Neophytos Lophitis is currently a Lecturer of Electrical Engineering at Coventry University. He is also an Academic Collaborator with the High Voltage Microelectronics laboratory within the Department of Engineering, Electrical Division, of the University of Cambridge. He received the B.A. and M.Eng degrees in 2009 and the Ph.D degree in 2014, all from the University of Cambridge. His research activities are in optimization, design, degradation and reliability of high voltage microelectronic devices, electrical energy storage and conversion systems.

Jose A. Antonino-Daviu received his M.S. and Ph. D. degrees in Electrical Engineering, both from the Universitat Politècnica de València, in 2000 and 2006, respectively, as well as his Bs. in Business Administration in 2012. He was working for IBM during 2 years, being involved in several international projects. Currently, he is Associate Professor in the Department of Electrical Engineering of the mentioned University. He has been invited professor in Helsinki University of Technology (Finland) in 2005 & 2007, Michigan State University (USA) in 2010, Korea University (Korea) in 2014 and Université Claude Bernard Lyon 1 (France) in 2015. He is IEEE Senior Member and has published over 160 contributions, including international journals, conferences and books.

Konstantinos N. Gyftakis was born in Patras, Greece, in 1984. He received the Diploma in Electrical and Computer Engineering from the University of Patras, Greece in 2010. He pursued a Ph.D in the same institution in the area of electrical machines condition monitoring and fault diagnosis (2010-2014). Then he worked as a Post-Doctoral Research Assistant in the Dept. of Engineering Science, University of Oxford, UK (2014-2015). Since 2015, he is a Lecturer in the Faculty of Engineering, Environment & Computing of Coventry University. His research activities are in fault diagnosis, condition monitoring and degradation of electrical machines. He has authored/co-authored more than 60 papers in international scientific journals and conferences.